

## **Responses to the Comments of Reviewer #2**

Thank you for your constructive suggestions, which is very useful for improving the readability of the manuscript. We have carefully addressed all the comments and suggestions you raised and provided a point - by - point response to each comment as follows. The revised manuscript looks like a new submission. The queries posed by the reviewer are presented in black text, the corresponding responses are showed in red text, and the revised content in the manuscript is in blue text.

### **General Comments**

1. Most of my comments pertain to the language presented in the manuscript. I understand that English is not everyone's first language, and I apologize in advance if my remarks come across as insensitive in any way. I strongly recommend that the authors have this manuscript proofread by someone proficient in English. Doing so will help elucidate some of the language used and improve the overall quality of the manuscript. Please note that some aspects of the research presented here are outside my area of expertise, so I apologize in advance if any of my comments seem basic.

**Response:** We express our sincere gratitude for your suggestions, which are of great significance for enhancing the quality and readability of the manuscript. The manuscript was meticulously proofread by individuals proficient in English, which contributed to clarifying certain language usage and elevating the overall quality of the manuscript.

2. Data and Methods: I believe this section needs substantial revision, particularly with regard to:

- Site and instrumentation description
- Data utilization and quality control, in particular:
  - o Validation of deployed instrument measurements to ground based instruments
  - o Quality control techniques
- Analysis techniques in sections detailing:
  - o K-means cluster analysis

o Utilization of turbulence parameters

**Response:** We express our sincere gratitude for your constructive suggestions, which have proven highly valuable for the enhancement of our manuscript. In the revised version, the section titled “Data and Methods” has been comprehensively rewritten and reorganized, and it is now divided into the following sub - sections. The specific details can be found within the revised main body of the text.

2.1 Experimental setup and data collection

2.1.1 Experimental setup

2.1.2 Data collection and quality control

2.2 Methods

2.2.1 Identification of potential source regions for BC and BrC

2.2.2 K-means cluster analysis

2.2.3 Utilization of turbulence parameters

3. Results:

- In the manuscript, some figures are referenced with variables that do not appear in the figures themselves. For example, the manuscript mentions a height reference to Figure S1, but the figure does not contain any height dimension.

- I believe that some figures in the supplement should be included in the manuscript itself. For example, Figure S1 is referenced frequently in alongside Figure 3. It makes it easier to read and understand when both figures are present the manuscript rather than having to reference the supplement section for figures.

**Response:** We express our sincere gratitude for your constructive suggestions. These suggestions are of great significance for enhancing the readability of our manuscript. In accordance with your suggestions, all figures have been reorganized and redrawn, and variables that do not appear within the figures themselves have been added. In Figures 3, 4, and S3, the size of the squares or dots represents altitude, with the altitude ranging from 0.65 to 2.70 km as the size of the squares or dots increases. Figure S1 in the supplementary information has been relocated to the main text and renamed as Figure 3, and the former Figure 3 has been renamed as Figure 4.

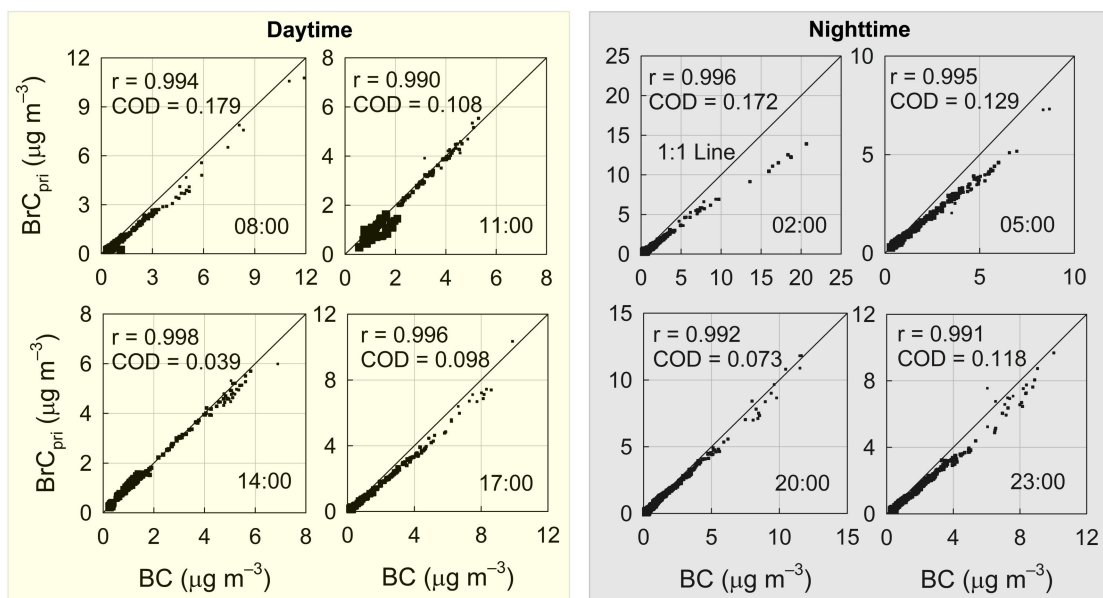


Fig. 3 Diurnal variations in the relationships between the profiles of BC and BrC<sub>pri</sub> during the campaign. The correlation coefficients ( $r$ ) exceed 0.99 for all the relationships. The coefficients of divergence (COD) were calculated using the following equation:  $COD_{jk} = \sqrt{1/p \times \sum_1^p [(x_{ij} - x_{ik}) / (x_{ij} + x_{ik})]^2}$ . The black solid lines represent the 1:1 line. The situations during daytime (08:00, 11:00, 14:00, and 17:00, local time) and nighttime (02:00, 05:00, 20:00, and 23:00) were delineated by transparent yellow and gray boxes, respectively. The size of the squares signifies altitude, with the altitude ranging from 0.65 to 2.70 km as the squares increase in size.

### Major comments

1. Abstract (Lines 32 - 50): Abstract needs to be rewritten, the language makes it a bit hard to follow. There are grammatical and sentence structure issues that I believe after resolving, can really improve the flow of the abstract and elucidate the content for the reader.

**Response:** I express my gratitude for your suggestions. The abstract has been rephrased, and several key actual findings have been incorporated into the revised abstract. Moreover, the grammatical and sentence structure issues in the abstract have been addressed in the revision, which is presented in blue text as follows.

The comprehension of the influence of planetary boundary layer (PBL) processes on the vertical profiles of air pollutants in complex terrains remains highly restricted. In this study, data from the First Planetary Boundary- Layer Meteorology and Pollution campaign in the western Sichuan Basin (1<sup>st</sup> BLMP - SCB), carried out from December 2018 to January 2019, are utilized. The focus of the campaign is to provide data on the impact of the elevated turbulence on the profiles of particulate matter (PM) pollutants. This study focuses on two types of PM: black carbon (BC), as well as brown carbon from primary sources ( $\text{BrC}_{\text{pri}}$ ) and that formed through secondary processes ( $\text{BrC}_{\text{sec}}$ ). The concentrations of BC and  $\text{BrC}_{\text{pri}}$  demonstrate a rapid decline as altitude increases, whereas the vertical profile of  $\text{BrC}_{\text{sec}}$  concentration is variable. The results of k - means clustering reveal three distinct types of vertical profiles of  $\text{BrC}_{\text{sec}}$ : (1) relatively uniform vertical distributions (accounting for 17.28% of all profiles), (2) higher values at an altitude of 1.4 km above sea level (ASL) (16.05% of all profiles), and (3) more rapid decreases with the increase in altitude (66.67% of all profiles). Further analysis demonstrated that the nocturnal concentration profiles of  $\text{BrC}_{\text{sec}}$  exhibit greater uniformity, featuring a minor peak at altitudes exceeding 1.7 km ASL. These profiles are more significantly influenced by thermodynamic processes. During the daytime,  $\text{BrC}_{\text{sec}}$  is mixed downward into the PBL through dynamic processes, namely, the elevated mechanical turbulence induced by wind shear. Throughout the campaign, both BC and  $\text{BrC}_{\text{sec}}$  exhibit comparable regional and long-range transport characteristics. This study emphasizes the significance of the elevated turbulence in shaping the vertical profiles of PM pollutants in complex terrains. Specifically, the results are helpful for understanding formation mechanism of heavy air pollution within these complex topographic environments.

2. All Figures in manuscript: Text on the figures are too small and hard to look at initially for information. For example: Figures 4, 5, S4, and S5 have embedded text that is critical for interpreting the figures, but the small text make this difficult. I recommend enlarging the text in all figures for better clarity.

**Response:** Thank you for your constructive suggestions. The embedded text within all figures has been enlarged to enhance clarity.

3. Lines 134 - 135: “The first field campaign of Boundary Layer Meteorology and Pollution at SiChuan Basin (BLMP-SCB) was conducted at a rural site (Sanbacun, 103°40’38” E, 30°54’59” N) of eastern foothills of Tibetan Plateau in winter of 2018, lasting about 40 days (Fig. 1).” - Please include elevation for those not familiar with the region.

**Response:** Thank you for identifying that issue. The statement “... at a rural site (Sanbacun, 103°40’38” E, 30°54’59” N) ...” has been amended to “... at a rural site (Sanbacun, 103°40’38” E, 30°54’59” N, 650 m) ...”. The elevation of Sanbacun has been incorporated into the revised version of our manuscript.

4. Lines 146 - 147: “The performances of the sensors were verified by comparing with on-ground reference instruments (Pang et al., 2021) ...” - What instruments specifically? Can you provide some statistics describing these differences? (For example: R<sup>2</sup>)?

**Response:** I sincerely appreciate your reminder. The sentences in Lines 146 - 147 have been revised in accordance with your suggestions. The revised contents are presented in blue text as follows.

The performance of the package (gaseous and particulate matter sensors) was validated through comparison with on - ground reference equipment (Model 49C, Model 42i, Model 450i, Model 48i - TLE, Model 5030i, Thermal Fisher, USA) with coefficients of determination (R<sup>2</sup>) ranging from 0.81 to 0.93 (Pang et al., 2021).

5. Lines 168 - 170: “The radiosonde has been widely used and validated (Haman et al., 2012), and there is a very slight difference with the other radiosondes such as Vaisala RS92 (Trapp et al., 2016).” – Validated how? Again, I think providing quantitative statistics that describe the difference would be beneficial.

**Response:** Thank you for your suggestions. The sentences in Lines 168 - 170 have been revised in accordance with your suggestions. The revised contents are presented in blue text as follows.

The radiosonde has been extensively utilized and verified (Haman et al., 2012), and there exists a negligible disparity compared to other radiosondes, such as the Vaisala RS92 (Trapp et al., 2016). The iMet-1 AB radiosonde and the Vaisala RS92 radiosonde were attached to the same 200-g balloon and launched from the identical location during the daytime. The measurements obtained from the two radiosondes exhibited extremely minor disparities in temperature. Specifically, the median difference remained below 0.5 K across all altitudes below 200 hPa. The RH measured by the iMet radiosonde exhibited a marginal decrease within the boundary layer (median values approximately -2%) and a slight increase within the 500 - 300 hPa layer (median values approximately +2%). Nevertheless, overall, the disparities were negligible throughout the troposphere (Trapp et al., 2016).

6. Lines 217 – 219: “Clustering analysis was used to divide the UVPM profiles during the campaign into three groups with comparable vertical structure of UVPM within groups.” – What are the groups? Explain in greater detail what each group signifies. How did you decide that three clusters were appropriate for this analysis? I suggest providing some sort of clustering validation to determine the correct number of clusters, such as “The Elbow Method” or even “Silhouette score” could be beneficial. I recommend the authors look into this and provide context, you do not necessarily need to provide plots, but I think a simple reference would suffice.

**Response:** We express our sincere gratitude for your constructive suggestions. These suggestions are of great significance in enhancing the readability of our manuscript. The characteristics of each cluster were presented in a table, and the number of clusters was determined using the Elbow Method. The relevant reference was provided in the revised manuscript. The relevant contents are presented in blue text as follows.

The determination of the number of clusters is crucial for attaining novel and accurate understandings. Drawing upon the Elbow Method (Syakur et al., 2018) and the characteristic profiles of air pollutants, k - means clustering analysis was employed to partition the BrC<sub>sec</sub> profiles during the campaign into three clusters, with each cluster featuring a comparable vertical structure of BrC<sub>sec</sub>. The characteristics of each cluster of the BrC<sub>sec</sub> profile are presented in Table 2.

Table 2 Characteristics of the three clusters of BrC<sub>sec</sub> profiles.

Cluster	Descriptions	Frequency
1	Relatively uniform vertical distributions	17.28%
2	Higher values at an altitude of 1.4 km above sea level (ASL)	16.05%
3	More rapid decreases with the increase in altitude	66.67%

7. Lines 231 – 233: “The ONA algorithm results in significant noise reductions and much more reasonable temporal changes in mass concentrations of carbonaceous particles (Cheng and Lin 2013; Park et al., 2010).” – What exactly is the “ONA algorithm”? I think a more in-depth description into the mechanics and procedures of this algorithm is necessary. What percentage of data required the ONA technique? I think including this is also necessary to include in the manuscript for context.

**Response:** Thank you for your constructive suggestions. As you suggested, the highly simplistic depiction of the ONA algorithm impeded the comprehension of the technique. The revised explications are presented in blue text as follows.

The micorAeth MA200 might yield negative values under conditions of lower mass concentrations and higher temporal resolution, which can account for up to 30% of the uncertainty associated with the filter - based optical attenuation technique (Hagler et al., 2011). Consequently, the raw data acquired for vertical profiles must be

rectified prior to analyzing their characteristics, particularly for in - situ observations at high altitudes. The mere removal of negative values is an inappropriate approach, as it would neglect the corresponding positive fluctuations caused by noise and lead to an upward bias in the final data. Averaging data over an extended time frame typically mitigates the noise within the signal; however, this may conflict with the requirement for high temporal - resolution data. Post - processing strategies such as moving averages or advanced mathematical techniques can be utilized to isolate the noise and reconstruct the time series (Kostelich and Schreiber, 1993). Nevertheless, these methods fail to leverage the ATN values associated with the internal load rate of the filter and the knowledge regarding the successive difference characteristic of the MA200. The optical noise - reduction averaging (ONA) algorithm, devised by Hagler et al. (2011), aims to perform adaptive time - averaging of carbonaceous components so as to mitigate the noise in BC data.

The ONA algorithm conducts smoothing processing on the time series of carbonaceous particles via a user - specified minimum attenuation change ( $\Delta\text{ATN}_{\min}$ ). For a given concentration of carbonaceous aerosols, this process leads to an adjusted timebase ( $\Delta t'$ ). When the concentration reaches a sufficiently high level or the intrinsic timebase is long,  $\Delta\text{ATN}$  will exceed  $\Delta\text{ATN}_{\min}$ , and the intrinsic time resolution will be maintained. Nevertheless, in the case of relatively low concentrations or short timebases,  $\Delta\text{ATN}$  will be lower than  $\Delta\text{ATN}_{\min}$ , and the time series will be smoothed over the time intervals  $\Delta t' > \Delta t$  required to attain  $\Delta\text{ATN}_{\min}$ . A second constraint is that the ATN value at the conclusion of the interval  $\Delta t'$  must be the final instance of that value within the remaining part of the time - series for that specific sample spot. Consequently,  $\Delta t_i'$  is extended to the ultimate occurrence of that ATN value. The frequency of negative values is reduced by applying the constraint. This is because when the ATN value returns to the same level later in the time - series, it implies that  $\Delta\text{ATN} < 0$  at that specific time step, which leads to a negative concentration. A consequence of the second constraint is that a certain level of smoothing exists even when  $\Delta\text{ATN}_{\min}$  equals zero. In principle, the average



concentration of carbonaceous particles during the time interval  $\Delta t_i$  can be calculated using  $\Delta ATN_i/\Delta t_i$ . Nevertheless, the duration of light transmission measurement at a high temporal resolution is relatively brief, rendering it prone to noise interference. The mean concentration of carbonaceous particles during the time interval  $\Delta t_i$  is calculated by averaging the set of concentrations reported at the intrinsic timebase within that interval. The incidence of negative concentrations should be less than 30% of the datasets to guarantee data quality. This is a straightforward method for addressing the noise in real - time data from the micorAeth MA200. It achieves this by dynamically adjusting the competing factors of averaging time and noise, thereby preserving the highest possible temporal resolution within the datasets. The algorithm leads to substantial reductions in noise and considerably more rational temporal variations in the mass concentrations of carbonaceous particles (Cheng and Lin, 2013; Park et al., 2010). The program was employed to conduct post - processing on the negative values obtained from our real - time profile measurements.

8. Line 237: The authors mention UVPM<sub>pri</sub>, but do not reference what it is or what it means? I assume this means organic carbon from primary sources, but this is not directly stated in the prior sections.

**Response:** Thank you for your reminder. In fact, the ultraviolet particulate matter (UVPM) corresponds to brown carbon (BrC). Consequently, UVPM has been uniformly substituted with BrC across the entirety of the manuscript. Brown carbon stemming from primary sources and secondary formation has been respectively designated as BrC<sub>pri</sub> and BrC<sub>sec</sub>. These designations have been explicitly stated in the preceding sections of the revised manuscript.

9. Lines 252 – 254: At this stage in the manuscript, the distinction between UVPM<sub>pri</sub> and UVPM<sub>sec</sub> in Equations 1 and 2 is not clear to me. In Eq. 2 UVPM is referenced, but the manuscript does not specify how UVPM differs from UVPM<sub>pri</sub> and UVPM<sub>sec</sub>.

**Response:** I sincerely appreciate your attention to this matter. I deeply apologize for

the confusion arising from the ambiguous expression. In the revised manuscript, UVPM, UVPMpri, and UVPMsec have been respectively substituted with BrC, BrCpri, and BrCsec, and their definitions are provided upon their initial appearance. The revised text is presented in blue as follows.

The estimation of secondary brown carbon ( $BrC_{sec}$ ) holds significant importance in ascertaining the proportion of  $BrC_{sec}$  within BrC. Initially, the minimum ratio of BrC to BC, denoted as  $(BrC/BC)_{min}$ , was employed as a surrogate for the ratio of  $BrC_{pri}$  to BrC ( $BrC_{pri}/BrC$ ) to estimate the mass concentrations of  $BrC_{sec}$  (Castro et al., 1999). Nevertheless, numerous studies have indicated that the  $(BrC/BC)_{min}$  demonstrates a certain level of randomness in actual observations, which results in substantial errors, particularly for the low BC concentrations in high - altitude regions. To tackle this issue, Lim and Turpin (2002) put forward the approach of arranging the BrC/BC ratios in ascending order and substituting the  $BrC_{pri}/BC$  ratio with the mean value of the top 10%–20% of the data. However, there is a dearth of a universally applicable criterion for determining the appropriate percentile range. In light of the disparate sources of  $BrC_{sec}$  and BC, Millet et al. (2005) put forward a method for estimating  $BrC_{sec}$  concentrations by utilizing the minimum correlation coefficient between BrC and BC. This methodology aims to determine the  $BrC_{pri}/BC$  ratio (designated as  $(BrC/BC)_{pri}$ ) at which the correlation between  $BrC_{sec}$  and BC reaches its minimum, and this ratio is employed as the  $BrC_{pri}/BC$  ratio. Adopting this approach, Wu and Yu (2016) devised a toolkit within Igor Pro for calculating the mass concentration of  $BrC_{sec}$ . This development notably improved the precision of  $BrC_{sec}$  estimation, as presented in Eqs. (1) and (2).

$$BrC_{pri} = (BrC/BC)_{pri} \times BC, \quad (1)$$

$$BrC_{sec} = BrC - BrC_{pri}. \quad (2)$$

In Eq. (1),  $(BrC/BC)_{pri}$  denotes the ratio of the concentrations of  $BrC_{pri}$  to BC during the campaign. Based on the measurements of BrC and BC,  $BrC_{pri}$  and  $BrC_{sec}$  can be estimated by means of Eqs. (1) and (2).

10. Section 2.5 Calculation of mechanical turbulence and wind shear: It seems like the authors want to isolate shear as a main contributor to atmospheric exchange and transport. However, it is not clear to me how this is directly achieved. The authors mention the TKE equation and shear terms, but I recommend the authors look into the TKE Budget equation, if possible, given the instrumentation deployed and measurements available. The TKE budget equation provides more detailed insight into the generation, transport, and dissipation of turbulence across a specific transect.

**Response:** I express my sincere gratitude for your constructive suggestions, which have notably enhanced the readability of the manuscript. In accordance with the research findings of Lan et al. (2018) and Sun et al. (2012), the term “mechanical turbulence index” has been modified to “turbulent velocity scale” in the revised manuscript. As you suggested, The TKE budget equation offers a more comprehensive and in - depth understanding of the generation, transport, and dissipation of turbulence along a specific transect. In the context of unstable stratification, a significant correlation exists between TKE and the effects of mechanical shear and buoyancy (Yue et al., 2015). During the campaign, the buoyancy effect is notably suppressed on cloudy days (Song and Zhang, 2024). Furthermore, considering the constraints of the deployed instrumentation and the available measurements with relatively low temporal resolution, this study only analyzed the mechanical shear (including wind speed shear and directional shear). The revised contents were showed with the blue text as follows.

Turbulent kinetic energy (TKE) serves as an indicator of turbulence intensity, and it represents a crucial variable for the comprehension of the exchanges of energy, water vapor, and greenhouse gases between the land surface and the atmosphere. The turbulent velocity scale, defined as  $V_{TKE} = \left[ (1/2) (\overline{u^2} + \overline{v^2} + \overline{w^2}) \right]^{1/2} = \sqrt{TKE}$ , has been widely employed to characterize turbulence intensity (Lan et al., 2018; Sun et al., 2012). Here,  $u$ ,  $v$ , and  $w$  denote the zonal, meridional, and vertical wind components

respectively, while  $u'$ ,  $v'$ , and  $w'$  signify the standard deviation of each variable. The vertical profiles of  $V_{TKE}$  can be derived from the aforementioned equation. A positive correlation exists between the  $V_{TKE}$  and mechanical turbulence, such that an increase in  $V_{TKE}$  corresponds to an enhancement of mechanical turbulence. The combination of the profiles of  $V_{TKE}$  and air pollutants can be employed to gain a more comprehensive understanding of the downward transport of air pollutants at the eastern foothills of the Tibetan Plateau.

The TKE budget equation offers a more comprehensive and in - depth understanding of the generation, transport, and dissipation of turbulence along a specific transect (Martilli et al., 2002, Eq. 4).

$$\frac{1}{2} \frac{\partial e^2}{\partial t} = -\overline{u'w'} \frac{\partial \bar{u}}{\partial z} + \frac{g}{T} \left( \overline{w'\theta'} \right) - \frac{1}{2\rho} \frac{\partial \left( \overline{w'e^2} \right)}{\partial z} - \frac{1}{\rho} \frac{\partial \overline{w'p'}}{\partial z} - \nu \left( \frac{\partial \overline{u'_i}}{\partial x_j} \frac{\partial \overline{u'_i}}{\partial x_j} \right), \quad (4)$$

where  $e$  represents the TKE,  $t$  denotes time,  $g$  signifies the acceleration due to gravity,  $T$  stands for temperature,  $\theta$  represents the potential temperature,  $\overline{w'\theta'}$  refers to the turbulent heat flux,  $\overline{u'w'}$  indicates the turbulent momentum,  $\rho$  denotes the air density,  $u$  represents the wind speed,  $z$  represents the observational height,  $w'$  represents the vertical wind velocity fluctuation, and  $p'$  represents the atmospheric pressure pulsation. The value of TKE is primarily influenced by mechanical shear and buoyancy effects (represented by the first two terms on the right - hand side of Equation 4). In the context of unstable stratification, a significant correlation exists between TKE and the effects of mechanical shear and buoyancy (Yue et al., 2015). During the campaign, the buoyancy effect is notably suppressed on cloudy days (Song and Zhang, 2024). Furthermore, considering the constraints of the deployed instrumentation and the available measurements with relatively low temporal resolution, this study only analyzed the mechanical shear (including wind speed shear and directional shear).

11. Lines 310 – 312: “In order to better understand the mechanisms of the more

uniform profiles of UVP Msec as compared to those of BC and UVP Mpri, we firstly analyzed the relationships between UVP Msec or UVP Mpri and BC (Figs. 3 and S1).”

- This requires a bit of rephrasing to understand. The authors reference Figures 3 and S1 frequently in this section. I suggest moving Figure S1 into the main text. This just makes it easier to reference especially in a section of the results where both figures are needed together to clarify the interpretation.

**Response:** Thank you for your suggestions. In the revised manuscript, Figure S1 has been relocated to the main text and renamed as Fig. 3, whereas the former Fig. 3 has been renamed as Fig. 4. These two figures have been reorganized and redrawn to distinguish the situations between daytime and nighttime as well as different altitudes.

12. Lines 323 – 326: “Specifically, the differences between BC and UVP Mpri are getting smaller and smaller with the increasing altitudes at 02:00–11:00 and 23:00, while those are independent on altitudes with the low COD values (0.039–0.098) at 14:00–20:00 (Fig. S1).” – Authors mention altitude, but altitude is not on Figure S1.

**Response:** Thank you for your reminder. Figure S1 has been reorganized and redrawn to differentiate the scenarios between daytime and nighttime, along with those at different altitudes. The revised figure is presented in the aforementioned questions.

13. Lines 329 – 330: “During the daytime, UVP Msec firstly increased with BC concentrations and then decreased gradually as the increased BC.” – Rephrase, this is a bit confusing for the reader to understand.

**Response:** Thank you for your suggestions. The sentence in Lines 329-330 will be rephrased to “During the daytime, the  $BrC_{sec}$  exhibited an increasing trend with the rise in BC concentrations. Subsequently, as the BC concentrations continued to increase, the  $BrC_{sec}$  less varied.” in the revised version of our manuscript.

14. Lines 493 – 496: “. Furthermore, the UVP Msec peaks well correspond to the strong descending motion and wind shear, and thus the UVP Msec peaks at the upper air on 7 January 2019 are mainly modulated by dynamic processes instead of

thermodynamic processes.” – Not sure what “peak” is referenced here, not clear by looking at the figure(s).

**Response:** Thank you for your reminder. The figure has been modified to a time - height - concentration plot to facilitate the more straightforward discernment of the concurrent variations between the UVPMsec peaks, vertical motion, and wind shear. The revised Figure 8 is presented as follows.

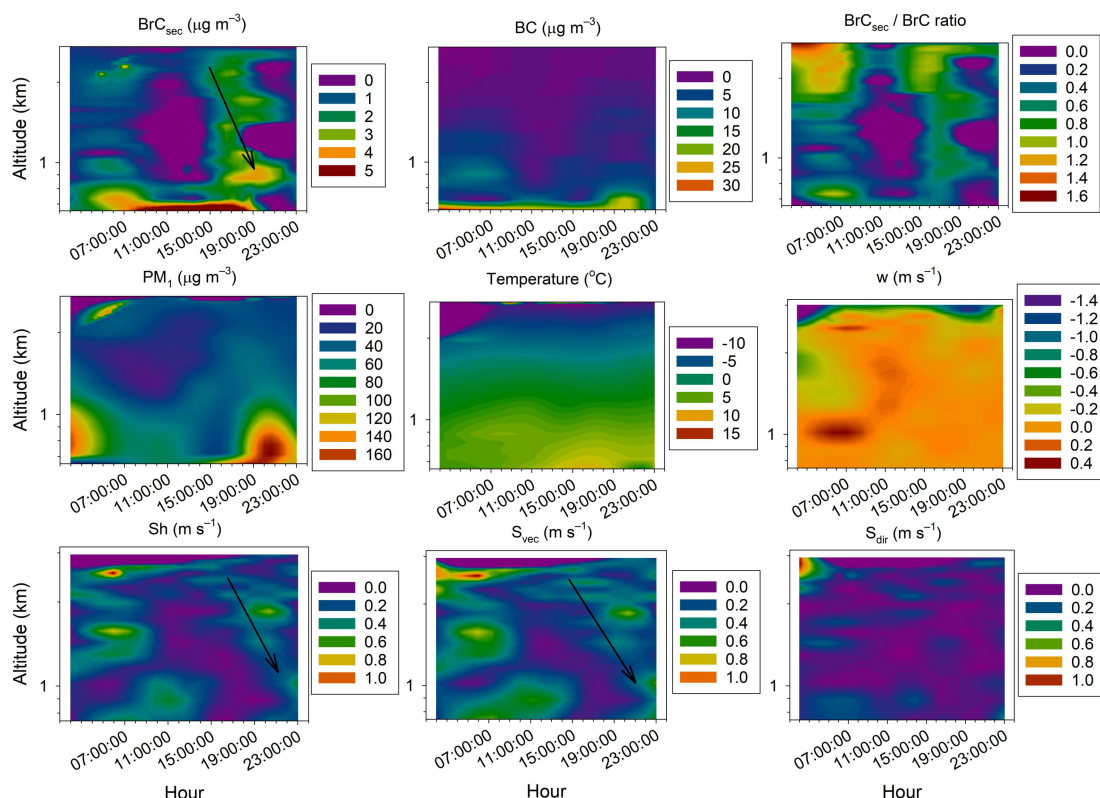


**Fig. 8** Diurnal variations in vertical profiles of air pollutants (BrC<sub>sec</sub>, BC, BrC<sub>sec</sub>/BrC ratio, and PM<sub>1</sub>) and meteorological factors (temperature,  $w$ , Sh,  $S_{vec}$ , and  $S_{dir}$ ) on 7 January 2019. The black arrows indicate the temporal movement of the peaks of profiles of BrC<sub>sec</sub>, Sh, and  $S_{vec}$ .

15. Lines 502 – 503: “As the surface is heated up and PBL developed during the daytime...” – I would suggest adding a plot that shows a time series of PBL development with height either from the Lidar or other remote sensing instruments (if possible). This helps visualize how deep and fast the PBL grows throughout the day.

**Response:** Thank you for your suggestions. The horizontal wind speed and direction,

as well as the vertical wind velocity, were observed on an hourly basis by a Doppler Wind Lidar at Sanbacun. The development of the PBL can be visualized through the diurnal variations of the vertical profiles of wind vectors within the x–y plane on 1 January 2019 (upper panel of Fig. S8). Moreover, the PBL height was calculated by means of the potential temperature gradient method using radiosonde data acquired from the tethered balloon, which is presented in the lower panel of Fig. S6. As can be discerned from the figure, the PBL developed rapidly after the early - morning hours (05:00), reached its maximum depth after noon (14:00), and subsequently declined gradually.

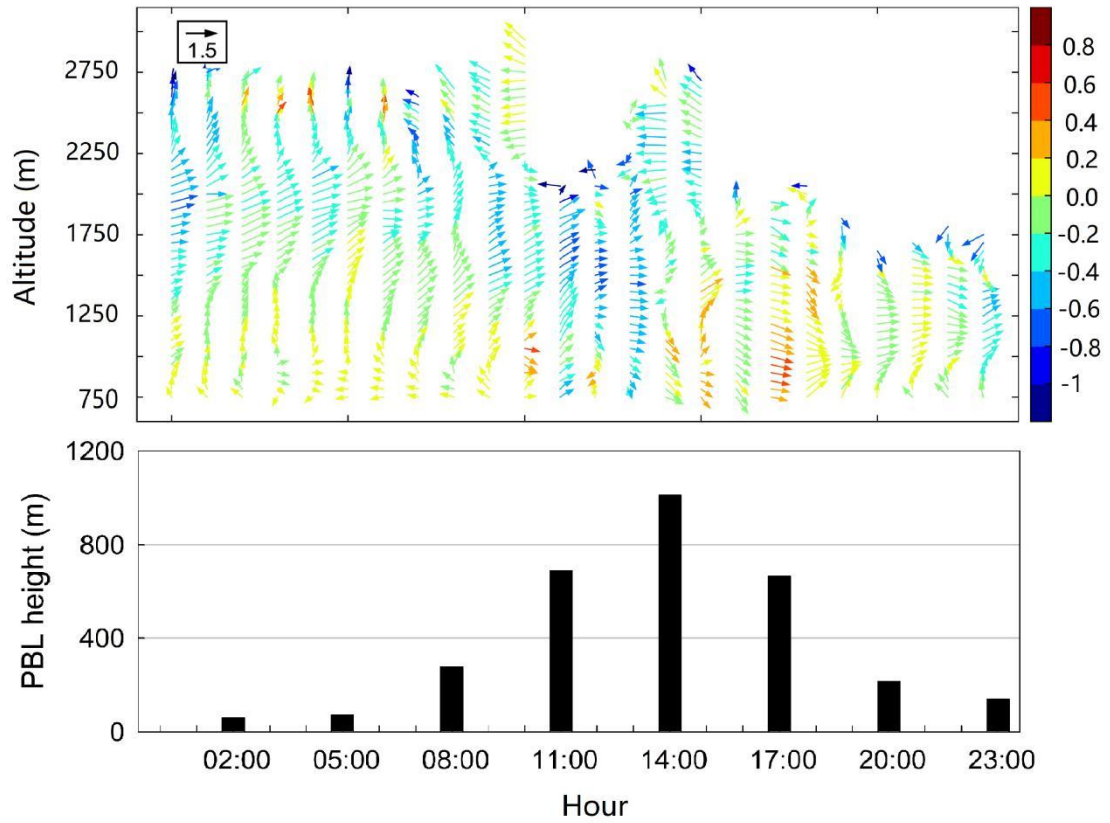


Fig. S6 Diurnal variations of the hourly vertical profiles of wind vectors within the x–y plane (upper panel) and the 3-h PBL height (lower panel) on 1 January 2019. The colors assigned to the wind vectors denote the vertical wind velocity ( $w$ ). The PBL height was calculated via the potential temperature gradient method using radiosonde data obtained from the tethered balloon ( $\frac{d\theta}{dz}|_{z=h_i}=0$ ).

### **Minor Comments:**

1. All figures: Figures that reference time (For example: Fig 3), are these all in local time? UTC?

**Response:** Thank you for your reminder. Throughout the manuscript, the local time (Beijing Time = UTC + 8) was utilized. This statement will be presented in the “2 Data and methods” section of the revised version of our manuscript.

2. Line 130: “... understanding the change in air pollutants and then taking targeted measures.” – What do you mean by “taking targeted measures”?

**Response:** I express my gratitude for your attention to this matter. The introduction section has been rewritten and reorganized in accordance with the theme of this study. Moreover, the statement “taking targeted measures” has been removed from the revised manuscript.

3. Lines 173 – 174: “The uncertainty of temperature and RH measurements was  $\pm 0.3$  °C and  $\pm 5\%$  given by the manufacturer.” – Provide citation of manufacturer.

**Response:** Thank you for your valuable suggestion. The sentence spanning Lines 173 - 174 has been revised to “The measurement uncertainties of temperature and relative humidity (RH) were  $\pm 0.3$  °C and  $\pm 5\%$ , respectively (Hosom et al., 1995)”. The relevant reference has been cited in the revised edition of our manuscript.

4. Line 183: “The DBS mode was used in this campaign.” – What is “DBS mode”? I suggest the authors describe this in greater detail. Provide citations.

**Response:** I sincerely appreciate your constructive suggestions, which are of great significance for enhancing the readability of the manuscript. During the campaign of the 1<sup>st</sup> BLMP-SCB, the Doppler beam swinging (DBS) mode was employed to present profiles of wind speed and direction. By shifting the beam among a series of four radial wind directions, which are generally at an elevation of approximately 60° and mutually perpendicular, the Doppler shift and consequently the line - of - sight



(LOS) velocity can be calculated for the DBS mode (Lundquist et al., 2015). Explanations will be incorporated into the revised manuscript.

5. Lines 189 – 191: What instruments were on the tower? Can you provide model #'s, also basic statistics on comparison between Lidar and sonic wind anemometer values?

**Response:** Thank you for your inquiries and recommendations. The revised content is presented in blue text as follows.

The wind data measured by the Lidar were verified through comparison with the on-site wind observations obtained by a sonic wind anemometer (Windmaster, Gill Instruments, Lymington, Hampshire, UK) installed on the Beijing 325 - m meteorological tower. The horizontal wind speed measurements obtained from the Doppler Wind Lidar exhibited a high degree of consistency with those acquired by the sonic wind anemometer, as evidenced by high coefficients of determination ( $R^2$ : 0.90–0.97). Furthermore, the results indicated a high degree of consistency between the two measurements of the dominant wind direction (Dai et al., 2020).

6. Lines 298 – 300: “Unlike UVPMpri profiles, the vertical distributions of secondary UVPM (UVPMsec) were more uniform, and the differences among the profiles were more significant than UVPMpri profiles.” – This is a bit unclear and should be rephrased for clarity.

**Response:** Thanks for your reminder. In the revised manuscript, the sentence spanning Lines 298 - 300 will be rephrased as follows for the sake of clarity: "In comparison with the profiles of  $BrC_{pri}$ , the profiles of  $BrC_{sec}$  exhibited greater uniformity, and the disparities among the  $BrC_{sec}$  profiles were more pronounced than those among the  $BrC_{pri}$  profiles at different time points."

7. Lines 346 – 348: “Fig. S3 showed the relationships between UVPMsec/UVPM ratio and UVPMpri or UVPMsec concentrations at the varying altitude ranges at the different times of the day.” – Rephrase for clarity. What do you mean by “UVPMpri

or UVPMsec”? Do you mean: “Figure S3 showed the relationships between the UVPMsec/UVPM ratio and UVPMpri, as well as between the UVPMsec/UVPM ratio and UVPMsec.”?

**Response:** Thank you for your suggestions. In the revised manuscript, the sentence in Lines 346-348 will be rephrased to “Figure S4 depicts the relationships between the ratio of BrC<sub>sec</sub> to BrC and BrC<sub>pri</sub>, as well as between the ratio of BrC<sub>sec</sub> to BrC and BrC<sub>sec</sub> concentrations across different altitude ranges at various time points throughout the day.” for clarity.

## Reference

Castro L.M., Pio C.A., Harrison R.M., Smith D.J.T., 1999. Carbonaceous aerosol in urban and rural European atmospheres: estimation of secondary organic carbon concentrations. *Atmospheric Environment*, 33(17), 2771–2781, DOI: 10.1016/S1352-2310(98)00331-8.

Cheng Y.H., Lin M.H., 2013. Real-time performance of the microAeth® AE51 and the effects of aerosol loading on its measurement results at a traffic site. *Aerosol and Air Quality Research*, 13(6), 853–1863.

Dai L.D., Coauthors, 2020. Multilevel validation of Doppler Wind Lidar by the 325 m meteorological tower in the planetary boundary layer of Beijing. *Atmosphere*, 11, 1051, doi:10.3390/atmos11101051.

Hagler G.S., Yelverton T.L., Vedantham R., Hansen A.D., Turner J.R., 2011. Post-processing method to reduce noise while preserving high time resolution in Aethalometer real-time black carbon data. *Aerosol and Air Quality Research*, 11, 539–546.

Haman C.L., Lefer B., Morris G.A., 2012. Seasonal variability in the diurnal evolution of the boundary layer in a near-coastal urban environment. *Journal of Atmospheric and Oceanic Technology*, 29(5), 697–710.

Hosom D.S., Weller R.A., Payne R.E., Prada K.E., 1995. The IMET (Improved Meteorology) ship and buoy systems. *Journal of Atmospheric and Oceanic Technology*, 12, 527–540.

- Lan C., Liu H., Li D., Katul G.G., Finn D., 2018. Distinct turbulence structures in stably stratified boundary layers with weak and strong surface shear. *Journal of Geophysical Research: Atmospheres*, 123, 7839–7854.
- Lundquist J.K., Churchfield M.J., Lee S., Clifton A., 2015. Quantifying error of lidar and sodar Doppler beam swinging measurements of wind turbine wakes using computational fluid dynamics. *Atmospheric Measurement Techniques*, 8, 907–920.
- Martilli A., Clappier A., Rotach M.W., 2002. An urban surface exchange parameterisation for mesoscale models. *Boundary-Layer Meteorology*, 104(2), 261–304.
- Millet D.B., Donahue N.M., Pandis S.N., Polidori A., Stanier C.O., Turpin B.J., Goldstein A.H., 2005. Atmospheric volatile organic compound measurements during the Pittsburgh Air Quality Study: Results, interpretation, and quantification of primary and secondary contributions. *Journal of Geophysical Research-Atmospheres*, 110(D7), D07S07, DOI: 10.1029/2004JD004601.
- Pang X.B., Chen L., Shi K., Wu F., Chen J., Fang S., Wang J., Xu M., 2021. A lightweight low-cost and multipollutant sensor package for aerial observations of air pollutants in atmospheric boundary layer. *Science of the Total Environment*, 764, 142828.
- Park S.S., Hansen A.D.A., Cho S.Y., 2010. Measurement of real time black carbon for investigating spot loading effects of Aethalometer data. *Atmospheric Environment*, 44, 1449–1455.
- Sun J., Mahrt L., Banta R.M., Pichugina Y.L., 2012. Turbulence regimes and turbulence intermittency in the stable boundary layer during CASES-99. *Journal of the Atmospheric Sciences*, 69(1), 338–351.
- Syakur M.A., Khotimah B.K., Rochman E.M.S., Satoto B.D., 2018. Integration K-means clustering method and Elbow method for identification of the best customer profile cluster. *2<sup>nd</sup> International Conference on Vocational Education and Electrical Engineering (ICVEE)*, 336, DOI: 10.1088/1757-899X/336/1/012017.
- Trapp R.J., Stensrud D.J., Coniglio M.C., Schumacher R.S., Baldwin M.E., Waugh S., Conlee D.T., 2016. Mobile radiosonde deployments during the mesoscale

predictability experiment (MPEX): rapid and adaptive sampling of upscale convective feedbacks. *Bulletin of the American Meteorological Society*, 97(3), 329–336.

Yue P., Zhang Q., Wang R., Li Y., Wang S., 2015. Turbulence intensity and turbulent kinetic energy parameters over a heterogeneous terrain of Loess Plateau. *Advances in Atmospheric Sciences*, 32, 1291–1302.